

Geophysical signatures of an urbanized floodplain: a case study at Tietê Ecological Park, São Paulo, Brazil

Dantas, L.R., USP; Ustra, A.T., USP; Barros, M.F.S., USP; Imbernon, R.A.L., USP; Stangari, M.C., USP; Santos, E.C., USP

Copyright 2023, SBGf - Sociedade Brasileira de Geofísica

This paper was prepared for presentation during the 18th International Congress of the Brazilian Geophysical Society held in Rio de Janeiro, Brazil, 16-19 October 2023.

Contents of this paper were reviewed by the Technical Committee of the 18th International Congress of the Brazilian Geophysical Society and do not necessarily represent any position of the SBGf, its officers or members. Electronic reproduction or storage of any part of this paper for commercial purposes without the written consent of the Brazilian Geophysical Society is prohibited.

Abstract

The critical zone is the region that encompasses the base of the water table and the top of the vegetation, where physical, chemical and biological processes interact through porous and reactive interfaces that transform and transmit flows of gases, energy and materials. Understanding its structure and dynamics can help in the development of predictive models, mainly in response to anthropogenic disturbances. However, predicting the CZ response to climate change and land use, and how they affect ecosystem services, requires an interdisciplinary and multi-technical approach. In this work, some results and preliminary interpretations of a medium-term study that is being carried out in the pilot observatory of the critical zone, in the region of Parque Ecológico do Tietê and Campus Leste USP, are presented. This is a region with a complex history of land use that is reflected in the variability of electrical resistivity and chargeability data.

Introduction

In 2001, the National Research Council defined the Earth's surface and shallow subsurface as a critical zone, whose boundaries are defined by the base of the water table and the top of vegetation (NRC, 2001), including the lower atmosphere. It is a laterally and vertically heterogeneous region, globally distributed, which covers environments with different physiographic characteristics such as geology, relief, climate, soils and their use types and vegetation cover. In the critical zone, the soil functions as a biogeochemical reactor (Banwart *et al.*, 2016), where physical, chemical and biological processes interact through porous and reactive interfaces that transform and transmit gases, energy and materials flows (figure 1).

Spatial and/or temporal variations of biogeochemical reactions and ecological functions are directly influenced by water flow (McClain *et al.*, 2003). These modifications depend on soil properties, such as pore size distribution and connectivity (Romero-Ruiz *et al.*, 2018) and redox dynamics (Zhang and Furman, 2021). These properties can be influenced by natural processes or anthropogenic disturbances, changing rates of processes and flows through the critical zone (Minor *et al.*, 2019) and propagating spatially and temporally at measurable scales.

Understanding the structure of the critical zone (CZ) and dynamics of interaction between biotic and abiotic processes can help in the development of predictive models, mainly in response to anthropogenic disturbances (Minor *et al.*, 2019; Waldron, 2020). Predicting the CZ response to climate change and land use, and how they affect ecosystem services, requires an interdisciplinary and multi-technical approach (Guo and Lin, 2016; Brantley *et al.*, 2017; Singha *et al.*, 2020). In this context, geophysical methods are important allies to interpolate and extrapolate data obtained by drilling holes (Riebe *et al.*, 2017).

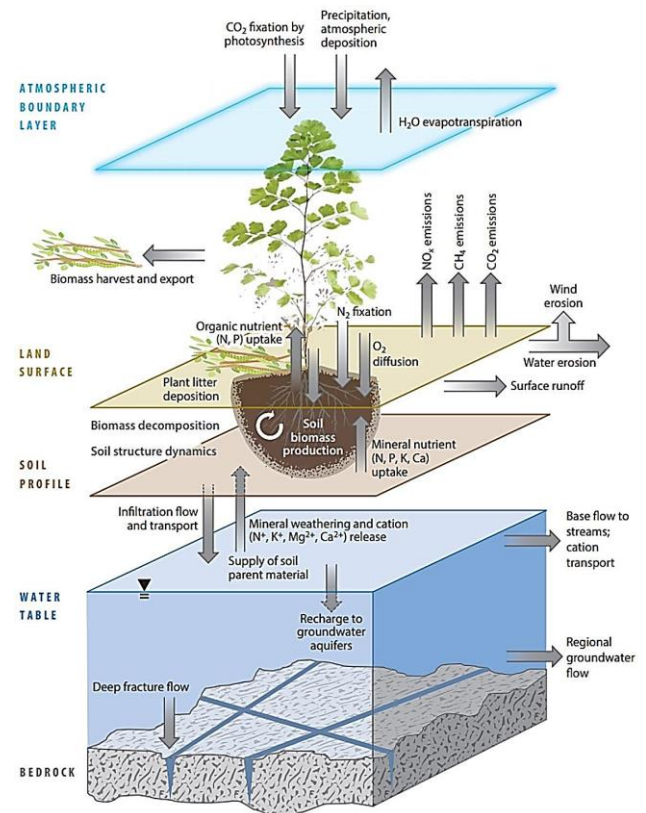


Figure 1 – Graphical representation of soil functions such as mass, energy and biodiversity flows within the Earth's critical zone (Banwart *et al.*, 2017).

The study area is located in the Tietê Ecological Park, an important leisure center in the eastern region of São Paulo city (figure 2). The park is part of the Environmental Protection Area of Varzea of Tietê River, marked by intense dynamics of land use and occupation. This resulted in a historical complex of contamination resulting from

agriculture, disposal of solid waste and deposition of sediments removed from the Tietê River channel, during its rectification (Mendonça *et al.*, 2015).



Figure 2 – Google map with study area localization (red polygon). The School of Arts, Sciences and Humanities of the University of São Paulo is represented by the white polygon.

This work is linked to the implementation of a critical zone pilot observatory at the School of Arts, Sciences and Humanities of the University of São Paulo, East Campus, and Tietê Ecological Park. It is a sustainable research framework integrating geophysical monitoring with hydrogeological and biogeochemical measurements to understand the impacts of seasonal processes on a contaminated urban environment in a subtropical climate. The main objective of this work is to present some preliminary results and interpretations for the park region.

Method

Two lines with a length of 112 meters were defined, one close to the Tietê River (red) and other more distant (yellow) (figure 3). In both, geophysical acquisitions were carried out and subsequent soil sampling and measurement of physical-chemical parameters of the water in the monitoring wells.



Figure 3 – Google map with geophysical acquisition lines and their respective monitoring wells, in the Tietê Ecological Park.

Electrical Resistivity (ER) and Induced Polarization (IP) methods

Resistivity and chargeability measurements in the time domain were obtained using the dipole-dipole arrangement (figure 4). In the July/22 acquisitions, Syscal and Elrec equipment (Iris-instruments) were used, programmed for 2s of current injection time and 180 ms of delay time, a 12 V battery and stainless-steel electrodes with a spacing of 5.0 meters. In November/22, the Supersting equipment was used for more automated data acquisition, in addition to changing the spacing between electrodes to 2.0 meters, in order to obtain greater detail in the sections.

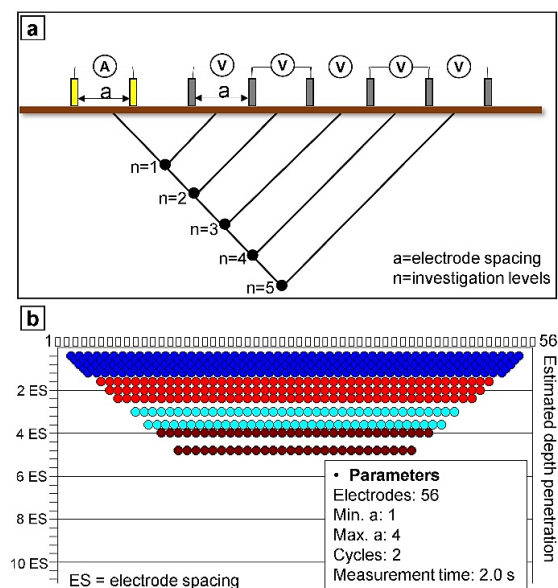


Figure 4 – a) Schematic drawing of the dipole-dipole arrangement; b) Structure of the command file inserted in Supersting for automated acquisition.

Pseudosections were generated from the inversion of the data acquired in the field, in the RES2DINV software (Iris-instruments) and the color scale was defined in a way to allow the comparison between the two acquisition lines. Initially, negative data and repeated measures were filtered, later, an inversion with smoothing link was performed.

Sampling

Two wells of 8.0 meters depth were drilled in the Tietê Ecological Park on the lines where geophysical monitoring is being carried out. The implantation of the wells followed the procedure established in the ABNT-NBR 15.495-1 Standard (2009 corrected version), using a dutch auger. Soil sampling was carried out during the installation of

monitoring wells, whose locations were defined from previous geophysical acquisitions. Soil samples were collected every 0.5 m, stored in plastic bags or in a liner. In situ measurement of physicochemical parameters of the water was also carried out. A Multiparameter Meter (Hanna) was used to measure pH, Electrical Conductivity, Oxidation-Reduction Potential, Dissolved Oxygen, Temperature and Turbidity.

Results

ER and IP acquisitions were carried out in July/ 2022 and November 2022 (figures 5 and 6). Apparent resistivity sections of both lines show a well-marked horizontal contrast, for both acquisition periods (figures 5a and 6a). In line 1, the values range from 21.2 ohm.m, around 7.0 meters deep, to 1317.7 ohm.m, closer to the surface. Values smaller than 12.1 ohm.m have a more restricted distribution at greater depths. In line 2, the horizontal resistivity contrast extends above 10.0 meters depth, with values ranging from 36.9 ohm.m, around 10.0 meters, to 572.4 ohm.m, closer to the surface.

Chargeability sections (figures 5b and 6b), show significant variation in the values, both depending on the acquisition period and the line. In July/2022 acquisitions (dry period), the depth of the horizontal contrasts in the chargeability sections is compatible with the resistivity sections. While, in the acquisitions of November/2022 (wet period), the contrasts are more discontinuous, showing a significant decrease in chargeability values. In line 1, the horizontal contrast surface presents values above 30.6 mV/V, while in discontinuous anomalies the values vary between 9.79 and 17.3 mV/V. In line 2, values above 30.6 mV/V are also observed, for the most continuous surface, while for punctual contrasts they show lower values, between 5.53 and 17.3 mV/V.

Figure 5 – Resistivity (a) and chargeability (b) sections of the PET (line 1) – Close to the Tietê River, obtained in July/22 and November/22. W.T. = water table.

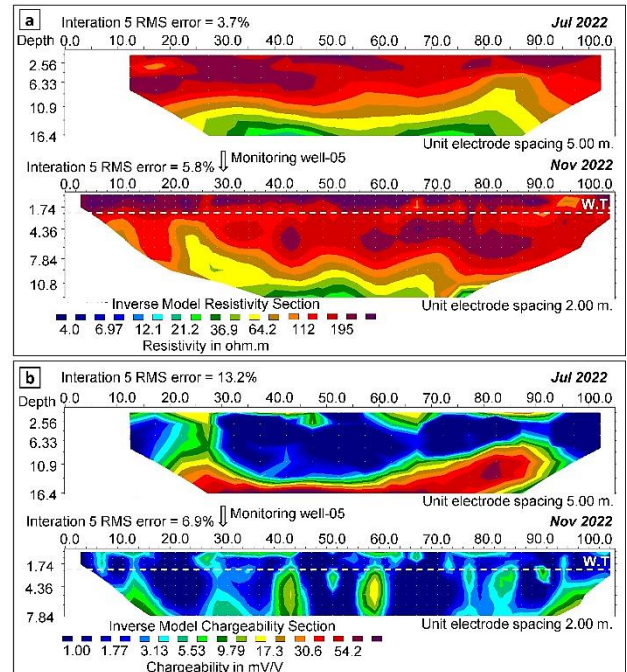
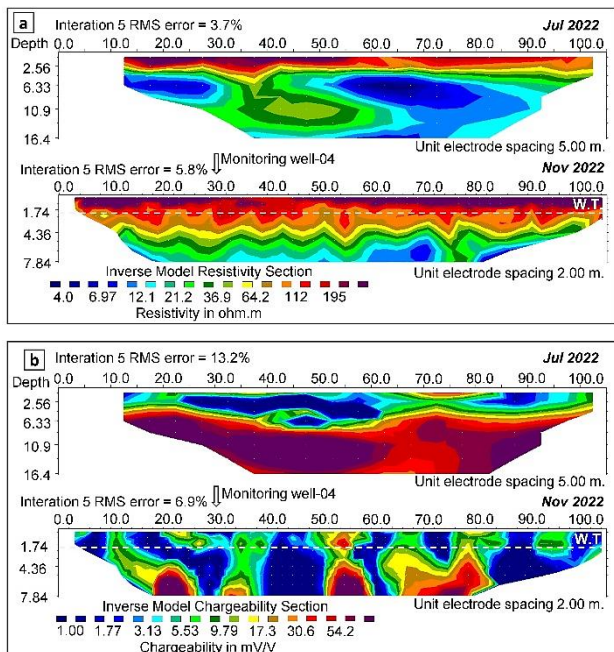


Figure 6 – Resistivity (a) and chargeability (b) sections of the PET (line 2) – Far from the Tietê River, obtained in July/22 and November/22. W.T. = water table.



In the monitoring wells, physical-chemical parameters and water table were measured for both lines. Both in line 1 well (PMN-04) and in line 2 well (PMN-05) the water level was identified close to 2.0 meters deep. Table 1 shows a significant variation in the electrical conductivity, redox potential and turbidity values. Both acquisition sites present a reducing behavior, however, with lower electrical conductivity and greater turbidity in the region of line 2.

Well	pH	EC (µS/cm)	ORP (mV)	DO (ppm)	T (°C)	Turbidity (NTU)
PMN 04	6,5	525	-99,4	< 0,5	21,5	190,0
PMN 05	6,2	267	-50,9	< 0,5	20,6	204,0

Table 1 – Physical-chemical data of water samples measured in November/2022. Electrical Conductivity (EC), Oxidation-Reduction Potential (ORP), Dissolved Oxygen (DO), Temperature (T).

The colors observed in the samples are compatible with sediment in a reducing environment, in the saturated zone.

Furthermore, description of the soil samples (table 2) shows the predominance of clayey material from 4.0 meters deep for line 1, which is compatible with the horizontal contrast observed in the resistivity (July and November/2022) and chargeability sections (July/2022). This interpretation is corroborated by the low values of electrical resistivity, associated with high values of chargeability, from 4.0 meters of depth. Shallower levels (up to 1.5 meters) are associated with higher resistivity values, being compatible with landfill. This material was also identified in previous environmental investigation studies carried out in the park (CONAM, 2017). However, the sections of line 2 show a more homogeneous behavior along the 8.0 meters of depth where the monitoring well is located. For both lines, it was also not possible to perform a satisfactory correlation between the soil sampling data and the geophysical acquisitions carried out so far.

Depth (m)	PMN-04		PMN-05	
	granulometry	color	granulometry	color
0.5	Clay, silt to fine sand with plant debris and rubble	Dark brown	Clay, silt to fine sand with plant debris and rubble	Dark brown
1.0	Clay, silt to fine sand with rubble		Clay, silt to fine sand with rubble	
1.5	Plastic clay to fine sand		Plastic clay to fine sand	
2.0	Clay to silt	Dark grey	Organic clay to fine sand	Dark grey
2.5	Plastic clay to fine sand		Plastic clay to fine sand	
3.0	Fine sand to clay	Light grey	Plastic clay to fine sand	Dark grey
3.5	Medium sand to pebble		Plastic clay to silt	
4.0	Clay, silt to fine sand	Light green	Medium sand to clay	Light green
4.5	Clay, silt to fine sand		Medium sand to pebble	
5.0	Clay, silt to fine sand		Coarse sand to pebble	
5.5	Clay, silt to fine sand		Clay, silt to fine sand	
6.0	Clay, silt to fine sand		Fine sand to clay	
6.5	Clay, silt to fine sand		Fine sand to clay	
7.0	Clay, silt to fine sand		Clay, silt to fine sand	
7.5	Clay, silt to fine sand		Clay, silt to fine sand	
8.0	Clay, silt to fine sand		Fine sand to clay	

Table 2 – Drilling profiles and classification of materials removed for installation of monitoring wells in November/2022.

Conclusions

This work presents some results and preliminary interpretations of a medium-term study that is being carried out at the pilot observatory of the critical zone, in the region of the Tietê Ecological Park and East Campus USP. This is a region with a complex history of land use that is reflected in the variability of electrical resistivity and chargeability data. Although the ER and IP sections present a certain correlation with the direct data, for line 1, the same does not occur for line 2. As the chargeability sections indicate a significant seasonal influence, further ER and IP acquisitions are needed, in addition to correlation with physicochemical parameters obtained in different periods, dry and rainy.

Acknowledgments

The authors acknowledge to Coordenação de Aperfeiçoamento de Pessoal de Nível Superior (CAPES), Fundação de Amparo à Pesquisa do Estado de São Paulo (FAPESP) process 2021/14808-6 and Living Lab EACH Project.

References

Banwart, S. A., Nikolaidis, N. P., Zhu, Y., Peacock, C. L., Sparks, D. L., 2016. Soil Functions: Connecting Earth's Critical Zone. Annual Review of Earth and Planetary Sciences. Doi: 10.1146/annurev-earth-063016-020544.

Banwart, S. A.; Bernasconi, S. M.; Blum, W. E. H.; Souza, D. M.; Chabaux, F.; *et al.*, 2017. Soil functions in Earth's critical zone: key results and conclusions. Advances in Agronomy, v. 142, p. 1–27.

Brantley *et al.* (11 co-authors), 2017. Designing a network of critical zone observatories to explore the living skin of the terrestrial Earth. Earth Surface Dynamics, vol. 5: 841–860, doi: 10.5194/esurf-5-841-2017.

CONAM - Consultoria Ambiental Ltda. Investigação ambiental detalhada, avaliação de riscos toxicológicos na Escola de Artes, Ciências e Humanidades da USP. Relatório técnico, 2017.

Guo, L. and Lin, H., 2016. Critical Zone Research and Observatories: Current Status and Future Perspectives. Vadose Zone Journal, vol. 15: 1-14, doi:10.2136/vzj2016.06.0050.

Mcclain, M.; Boyer, E.; Dent, C.; *et al.*, 2003. Biogeochemical Hot Spots and Hot Moments at the Interface of Terrestrial and Aquatic Ecosystems. Ecosystems, v. 6, p. 301–312, doi: 10.1007/s10021-003-0161-9.

Mendonça, C. A., Doherty, R., Fornaro, A., Abreu, E. L., Novaes, G. C., Fachin, S. S., La-Scalea, M. A., 2015a. Integrated earth resistivity tomography (ERT) and multilevel sampling gas: a tool to map geogenic and

anthropogenic methane accumulation on brownfield sites. *Environ Earth Sci*, 74, 1217–1226, <https://doi.org/10.1007/s12665-015-4111-6>.

Minor, J.; Pearl, J. K.; Barnes, M. L.; Colella, T. R.; Murphy, P. C.; Mann, S.; Barron-Gafford, G. A., 2019. Critical Zone Science in the Anthropocene: Opportunities for biogeographic and ecological theory and praxis to drive earth science integration. *Progress in Physical Geography*, doi: 10.1177/0309133319864268.

National Research Council, 2001. Basic research opportunities in the earth sciences. Natl. Acad. Press, Washington, DC.

Riebe, C. S.; Hahm, W. J.; Brantley, S. L., 2017. Controls on deep critical zone architecture: a historical review and four testable hypotheses. *Earth Surface Processes and Landforms*, v. 42, p. 128–156, doi: 10.1002/esp.4052.

Romero-Ruiz, A.; Linde, N.; Keller, T.; Or, D., 2018. A Review of Geophysical Methods for Soil Structure Characterization. *Review of Geophysics*, doi: 10.1029/2018RG000611.

Singha, K.; Sullivan, P. L.; Li, L.; Gasparini, N. M., 2020. Demystifying critical zone science to make it more inclusive. *Eos*, v. 101, doi: 10.1029/2020EO148937.

Waldron, P., 2020. Critical zone science comes of age. *Eos*, v. 101, doi: 10.1029/2020EO148734.

Zhang, Z.; Furman, A., 2021. Soil redox dynamics under dynamic hydrologic regimes - A review. *Science of the Total Environment*, v. 763, doi: 10.1016/j.scitotenv.2020.143026.